ORIGINAL ARTICLE

Estimation of Dose Perturbation Due to the Presence of Metal Hip Prostheses in Radiotherapy with Electron and Photon Beams: A Monte Carlo Study

Morteza Hashemizadeh [1], Mansour Zabihzadeh [1, 2, 3*], Omid Azadbakht [4], Masoud Jamali [5]

[1] *Department of Medical Physics, School of Medicine, Ahvaz Jundishapur University of Medical Sciences, Ahvaz, Iran*

[2] *Cancer Research Center, Ahvaz Jundishapur University of Medical Sciences, Ahvaz, Iran*

[3] *Department of Clinical Oncology, School of Medicine, Golestan Hospital, Ahvaz Jundishapur University of Medical Sciences, Ahvaz, Iran*

[4] *Department of Radiology Technology, Behbahan Faculty of Medical Sciences, Behbahan, Iran*

[5] *Radiation Oncologist, Technical Manager in Sarerm Hospital, Tehran, Iran*

*Corresponding Author: Mansour Zabihzadeh
Email: manzabih@gmail.com

Received: 11 November 2023 / Accepted: 22 December 2023

Abstract

Purpose: The impact of various hip prosthesis materials on the amount of dose perturbation generated by 9 MeV electron and 18 MV photon beams during pelvic radiation therapy is analyzed in this research.

Materials and Methods: The Varian 2100 C/D LINAC head for the electron (9 MeV) and photon (18 MV) modes and a water phantom with a realistic hip prosthesis were modeled using the Monte Carlo (MC) code; MCNPX (Ver. 2.6.0) and were benchmarked for measurement. Four different materials, including Cobalt–Chromium–Molybdenum-alloy (CCM), Stainless Steel (SS), Titanium, and Titanium-alloy (Ti-alloy) were evaluated. The changes in electron and photon fluences and dose perturbations due to the presence of the hip prostheses were investigated.

Results: An increased dose of 13.29%, 13.77%, 6.16%, and 5.93% for 9 MeV and 30.43%, 33.05%, 10.89%, and 11.27% for 18 MV was calculated for Ti-alloy, Ti, CCM, and SS prosthesis, respectively. At 0.5 mm distance from the prosthesis, the Electron Backscatter Factor (EBF) of 1.31, 1.33, 1.15, and 1.14 for 9 MeV and 1.32, 1.34, 1.11, and 1.12 for 18 MV was calculated for Ti-alloy, Ti, CCM, and SS prosthesis, respectively. Dose perturbation is higher at a near distance from the prosthesis; by reducing the distance from the Ti-alloy prosthesis (1.5 to 0.5 mm), an increased dose of 7.70% and 5.54% resulted in 18 MV and 9 MeV, respectively. The dose decreases of up to 21% behind the hip prosthesis were calculated for 18 MV.

Conclusion: It is essential to consider the dose perturbation due to the presence of a hip prosthesis to achieve the optimal treatment planning in radiotherapy.

Keywords: Dose Perturbation; Electron Backscatter Factor; Hip Prostheses; Monte Carlo Calculation; Radiotherapy.

DOI: https://doi.org/10.18502/fbt.v11i4.16513

1. Introduction

Most technical reports and guidelines propose precision and consistency in radiation dosimetry for the homogeneous medium; however, the human body includes components with different densities, such as teeth, bone, lungs, and air cavities inherent inhomogeneities in the human body. Additionally, biomaterials such as leg, arm, and hip prostheses, stents, surgical rods, spinal cord fixation devices, and different dental implants and fillings may exist in patients to carry out or support the function of human living tissues [1, 2].

The number of patients utilizing implanted hip prostheses has increased worldwide [3-5]; it was reported that 1% to 4% of patients who received radiation therapy have prosthetics [2]. These devices are usually made of elements with a high atomic number (high Z). They can significantly affect the absorbed dose by the target tissue and shielded or adjacent tissues in radiotherapy [1, 2]. Due to the best balance of resistance to fatigue, corrosion resistance, and mechanical strength, hip prostheses are made from Cobalt-Chromium-Molybdenum alloys (CCM). Both stainless steel and titanium hip prostheses are also available for clinical use [6-10]. It is anticipated that the number of people requiring prostheses will rise as the population ages due to malfunctioning hip joints and osteoarthritis, which might require partial or whole hip replacement. Leg sarcomas, rectal cancer, pelvic or pubic keloid lesions, and gynecologic malignancies may require therapeutic photon (for deep-located tumors) or electron (for superficial tumors) beam irradiation in the hip or pelvic regions [11, 12].

Radiation treatment planning of patients with hip prostheses exhibits two main obstacles; the high-Z material of the hip implant induces remarkable artifacts in the Computed Tomography (CT) images and shadowing for behind depths that play crucial roles in radiation treatment dose calculation [13, 14]. The inadequacies of the Treatment Planning System (TPS) in calculating the charged particle generation and photon scattering of various materials may lead to inaccuracies in dose calculation. As a result, excluding prostheses is recommended; however, this is not always practicable, and hence the accuracy of the TPS should be well-established by using correction factors to estimate the accurate dose distribution [1, 15-20]. The mega-voltage photon beam is usually used to deliver the prescribed dose to deep-depth tumors, while high-energy electron beams are used for superficial tumors. The typical electron beam energy in Intraoperative Electron Radiotherapy (IOERT) is a 9 MeV electron beam used in this study [21]. The typical external radiotherapy photon beam in the pelvic region is 15-20 MV [22].

The existence of a hip prosthesis potentially affects the dose distribution of electron or photon beams due to the high beam attenuation in the prosthesis and high backscattered electrons at interfaces. Knowing the amount of these dose perturbations is essential to planning a treatment plan with optimum dose distribution to deliver the maximum dose to the target volume (tumor) and minimum dose to Organs At Risk (OARs).

In this study, the Monte Carlo method is regarded as the gold standard method to calculate dose distribution in complicated cases in the presence of high atomic and density hip prostheses across the irradiated beam projection. The MCNPX 2.6.0 code was utilized to determine the dose perturbations caused by different hip prostheses in the presence of 9 MeV electron and 18 MV photon beams from the 2100 C/D Varian Linear Accelerator (LINAC). The resulting quantitative data was calculated and analyzed. Due to the lack of precise and limited information on dose perturbation due to the different hip prosthesis materials during electron or photon therapy, this study aims to simulate precise hip prosthesis with different materials and layers (Figure 1) to investigate the effect of different hip prosthesis on dose distribution during 9 MeV electron beam and 18 MV photon beam. The obtained results were systematically compared.

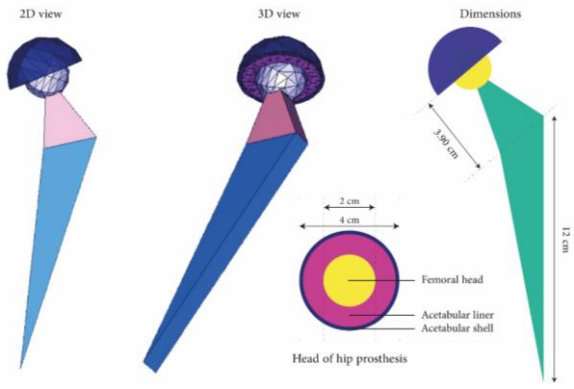

Figure 1. The model of the hip prosthesis

2. Materials and Methods

2.1. Benchmark the 2100C/D Varian LINAC Head (for 9 MeV and 18 MV)

In this study, 2100 C/D Varian LINAC head was simulated precisely for electron and photon modes with all components such as electron source, target (for photon mode), primary collimator, vacuum window, scattering foil and applicator (for electron mode), flattening filters (for photon mode), ionizing chamber, mirror, and secondary collimator by MCNPX 2.6.0 code (Figure 2). 9 MeV electron beam and 18 MV photon beam for Source-Surface-Distance (SSD) of 100 cm and field size of 10×10 cm^2 were modeled. The initial electrons were set to 2×10^9 for both electron and photon beams. The water phantom was simulated with a $50 \times 50 \times 50$ cm^3 dimension. The voxel size was set to $0.1 \times 0.1 \times 0.1$ cm^3 dimensions for calculating PDD and profile dose for benchmarking of 9 MeV electron beam and 18 MV photon beam. The 9 MeV electron beam dose profile was calculated at a depth of R50 which the absorbed dose falls to 50% of the maximum dose. The 18 MV photon beam dose profile was calculated at a depth of 10 cm. The energy cut-off for photon and electron beams was 0.01 and 0.1 MeV, respectively [23, 24].

To ensure the accuracy of the MC modeled Varian LINAC's head, by the IAEA protocol TRS-398, PPD and dose profile measurements were taken using a 0.6 cc Farmer ionizing chamber (PTW, Freiburg, Germany) for both 18 MV photon and 9 MeV electron beams from the 2100C/D Varian LINAC with 10×10 cm^2 field size. The measurements were conducted at an IBA blue phantom (IBA dosimetry Schwarzenbruck, Germany) using the Scanditronix Wellhofer dosimetry system and OmnoPro software (version 6.4) for ionization measurement. To ensure consistency, each measurement was repeated three times, and the average value was reported. This ensured the stability of the LINAC's output.

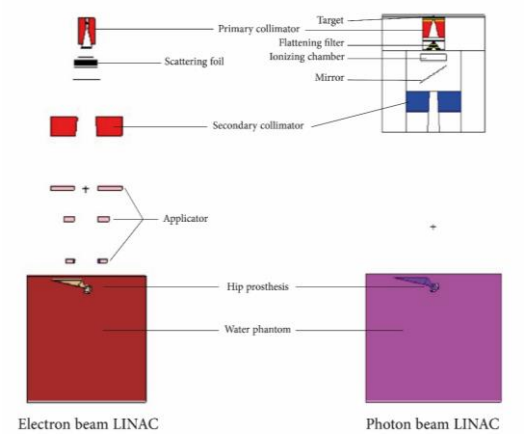

Figure 2. 2D view of Linac's heads for electron and photon modes. The hip prosthesis head is positioned at a 5 cm depth in the water phantom

2.2. Hip Prosthesis Simulation and Dose Calculation

The hip prosthesis includes three different layers that were simulated accurately. The main type of hip prosthesis simulated was Metal-on-Polyethylene (MoP). This prosthesis had different parts; femoral head and stem, acetabular liner, and acetabular shell. Polyether-Ether-Ketone (PEEK) was used for the acetabular liner. The center of the radiation field was adjusted to match the center of the hip prosthesis head which was positioned 5 cm deep in a water phantom. Figure 2 presents a diagram of the hip prosthesis, with Table 1 indicating the diverse materials utilized for the femoral head, acetabular shell, and stem.

Table 1. Mass density and elements Weight Fraction (WF) of the hip prosthesis materials

Ti $\rho = 4.506$ (g/cm^3)		**Ti alloy** $\rho = 4.48$ (g/cm^3)		**Stainless Steel** $\rho = 6.45$ (g/cm^3)		**Cr-Co-Mo alloy** $\rho = 8.20$ (g/cm^3)	
Element	WF (%)	Element	WF (%)	Element	WF (%)	Element	WF (%)
Ti	100	Ti	89.17	Fe	62.72	Co	61.90
-	-	Al	6.20	Cr	21.00	Cr	28.00
-	-	V	4.00	Ni	9.00	Mo	6.00
-	-	Fe	0.30	Mn	3.60	Mn	1.00
-	-	O	0.20	Mo	2.5	Si	1.00
-	-	C	0.08	Si	0.75	Fe	1.00
-	-	N	0.05	N	0.43	Ni	0.75
-	-	-	-	-	-	C	0.35

The voxel dimension was set to 5 × 5 × 1 mm^3 to calculate PDD. For each MC program, 2 × 10^9 initial electrons were transported to calculate fluences and absorbed doses to reach acceptable relative error. All relative error was less than 2 %. The Electron Backscatter Factor (EBF) [25] at the entrance side of the high-Z material can be calculated using the following (Equation 1):

$$EBF = \frac{D_2}{D_1} \quad (1)$$

D_2 and D_1 are the doses with and without the prosthesis, respectively.

3. Results

To achieve the most accurate results in the 9 MeV beam standard electron mode of LINAC, we carefully selected an incident electron beam with an asymmetric Gaussian distribution and left Full Width at Half Maximum (FWHM) energy spectra of 2.5 and 2.2 MeV through a process of trial and error. This approach ensured the best possible agreement between our measurements and MC calculations. The maximum relative error of MC calculations was less than 0.5% for PDD curves, which is well below the recommended value of 2%, demonstrating the high level of precision we achieved. The 18 MV photon beam was created by setting the incident electron beam to an average energy of 18.1 MeV. The energy distribution was Gaussian with an FWHM of 0.6 MeV, while the lateral intensity spread had an FWHM of 0.1 cm. The statistical uncertainty of the PDD curves was found to be less than 1%. The gamma index, which was estimated to be less than 1, indicates a good match between the MC-calculated and measured PDDs. Any small discrepancies observed may be attributed to missing information about the geometrical or materials used in the LINAC's components. The results for benchmarking the LINAC's head are shown in Figure 3 (data was shown only for PDDs of 10 × 10 cm^2 field size).

The calculated PDD curves in the presence of different hip prostheses for 9 MeV electron and 18 MV photon beams were shown in Figure 4a and Figure 4b, respectively. The related data from the homogeneous water phantom are also included for better comprising. All data were normalized to the maximum related dose in a water phantom without prostheses.

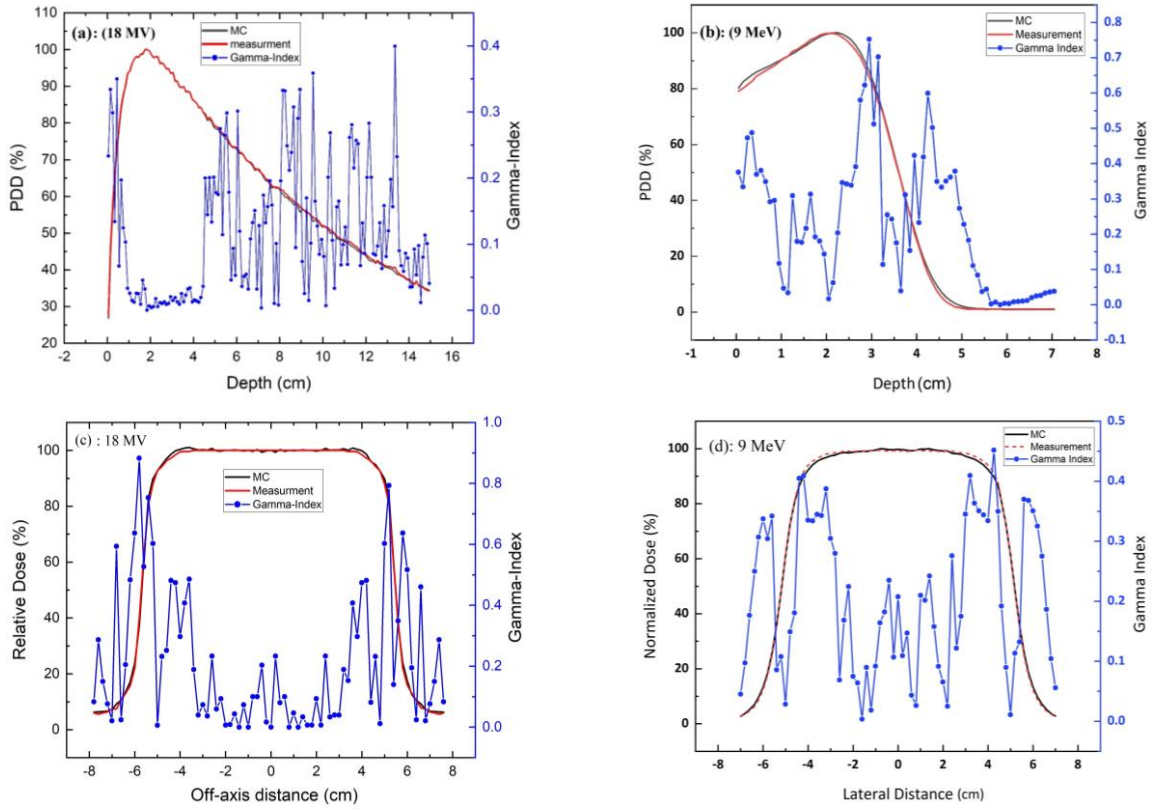

Figure 3. The comparison between measurement and Monte Carlo (MC) Calculated percentage depth dose (PDD) and profile dose; **(a, c)** for 18 MV beam, and **(b, d)** for 9 MeV beam of 10 × 10 cm^2 field size. The Gamma index (<1) shows a good agreement between measurement and MC calculation

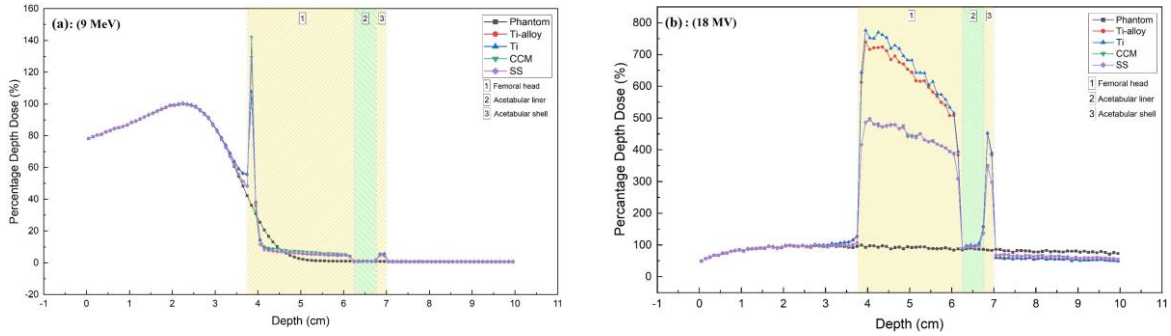

Figure 4. The percentage depth dose (PDD) curves in the presence of different hip prostheses for **(a)** 9 MeV electron and **(b)** 18 MV photon beams. All data were normalized to the maximum dose in water phantom without prostheses

Table 2 shows the increased doses and the EBFs in tissue at a distance of 0.5 and 1.5 mm in front of the prostheses. Maximum increased dose and EBFs for 18 MV and 9 MeV beams resulted from Ti prosthesis. Table 3 displays the results of various studies, providing a basis for comparison with the findings of the current study.

The electron and contaminant photon fluences for the 9 MeV electron beam were calculated; the electron fluence increased in front of the prosthesis (Figure 5a) while the contaminant photon fluence decreased (Figure 5b).

The photon and electron fluences for the 18 MV photon beam were calculated and are shown in Figure 6. As

Table 2. Increased dose (%) and Electron Backscatter Factor (EBF) at 0.5 mm and 1.5 mm distance in front of the different prostheses

Distance (mm)	Increased dose (%)							
	Ti-alloy		Ti		CCM		SS	
	9 MeV	18 MV	9 MeV	18 MV	9 MeV	18 MV	9 MeV	18 MV
0.5	13.29	30.43	13.77	33.05	6.16	10.89	5.93	11.27
1.5	7.75	22.73	8.12	24.33	3.03	8.63	2.87	9.09
	EBF							
0.5	1.31	1.32	1.33	1.34	1.15	1.11	1.14	1.12
1.5	1.16	1.25	1.17	1.26	1.06	1.09	1.06	1.09

Ti: Titanium / **CCM:** Cobalt–Chromium–Molybdenum-alloy / **SS:** Stainless Steel / **EBF:** Electron Backscatter Factor

Table 3. Our calculated increased dose (%) compared with the others reported data

9 MeV			18 MV		
Ref.	**Scattering interface**	**Dose perturbation (%)**	**Ref.**	**Scattering interface**	**Dose perturbation (%)**
Sathiyan *et al.* (2006) [26]	Al	8.5	**Çatlı *et al.* (2013) [1]**	Ti (PBC method)	6.2
	Cu	24		Ti (MC method)	7.2
	Pb	55		Ti-alloy (PBC method)	4
Das *et al.* (2004) [32]	Al	35		Ti-alloy (MC method)	6.5
	Ti	40		SS (PBC method)	17.2
	Cu	44		SS (MC method)	8.7
This study	Ti-alloy	13.30	**This study**	Ti-alloy	30.43
	Ti	13.77		Ti	33.05
	CCM	6.16		CCM	10.89
	SS	5.93		SS	11.26

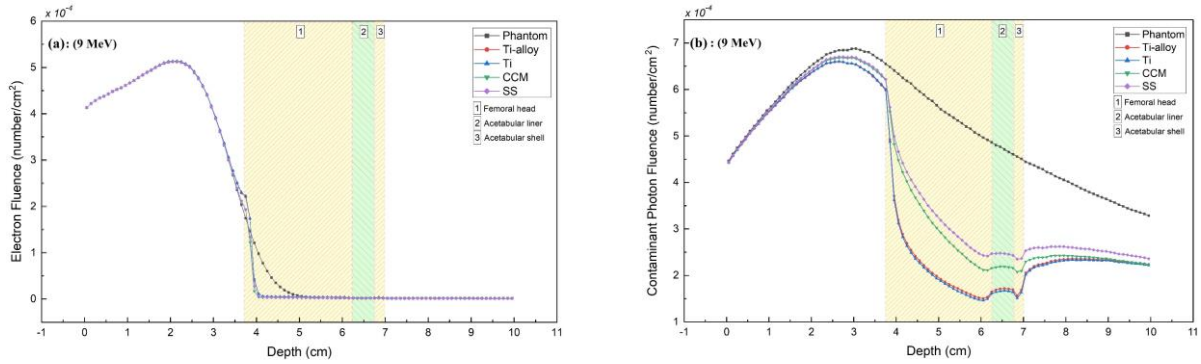

Figure 5. (a) The electron and **(b)** contaminant photon fluences for 9 MeV electron beam

expected for TI and Ti alloy prostheses, the photon fluence was lower in front of the prosthesis (Figure 6a), while electron production was higher (Figure 6b).

4. Discussion

In this study, the dose perturbation of four different hip prosthesis materials with different mass densities and atomic numbers have been quantified and evaluated for 9 MeV electron and 18 MV photon beams by MC calculation. It has been reported that photon beams can encounter limitations in the TPS algorithms when dealing with adjacent atomic numbers at the interfaces of hip prostheses. It has been reported that photon beams can encounter limitations in the TPS algorithms when dealing with adjacent atomic numbers at the interfaces of hip prostheses [7]; the available TPS does not provide electron scattering at tissue-prosthesis interfaces [11, 26]. For the 9 MeV beam, the contaminant photon fluence was decreased in front of the prosthesis with high atomic number and mass density (Figure 5b). Contaminant photon fluences were reduced in the prosthesis with a high density and atomic number due to increased photoelectric interaction probability compared to Compton interaction probability. Furthermore, an increase in contaminant photon absorption in the implant and, consequently, a decrease in photon scattering at the front depth of the implant is expected. As the prosthesis's atomic number and mass density increase, more absorbed photons decrease the photon fluence. Our data shows that Ti and Ti alloys produce lower contaminant photon fluences. For the 18 MV photon beam (Figure 6), SS and CCM prostheses with lower density and atomic number have higher photon fluences due to increased Compton interaction probability. At the same time, Ti and Ti alloys produced higher electron fluences.

Our data were calculated for the head of the hip prosthesis centered on the beam's central axis; which part of the hip prosthesis is placed in the center of the field will affect the shape of the dose distribution. According to research, high-Z materials have a more significant electron scattering cross-section, which means that a lower thickness of inhomogeneity is needed to reach the saturation value of EBF compared to low-Z materials [26]. In the in front of inhomogeneity region, the dose distributions are strongly dependent on the density of the inhomogeneity. For both electron and photon beams, the increase in EBF for the high Z-materials depends on the mass density of the prosthesis due to the higher scattering cross-section of primary and secondary electrons [27, 28].

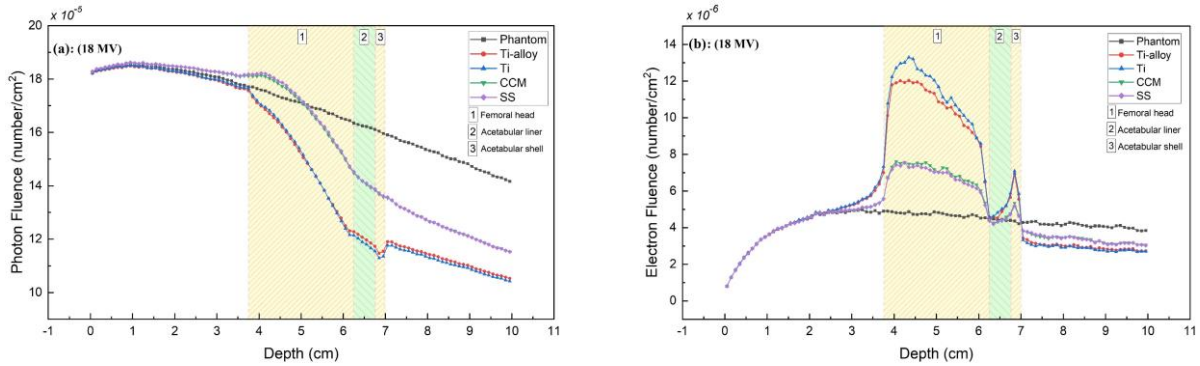

Figure 6. (a) The photon and **(b)** The electron fluences for 18 MV photon beam

The dose perturbation in the tissue adjacent to the prosthesis depends on the distance from the prosthesis, as seen in Figure 5b and 6b, electron or contaminant electron fluence is higher close to the prosthesis due to more backscattered electrons from the prosthesis; consequently, reducing the distance from the prosthesis increases the dose perturbation (Table 2). In the case of the prosthesis with Ti alloy, decreasing the distance from the prosthesis (from 1.5 mm to 0.5 mm), an increased dose of 7.70% and 5.54% resulted in 18 MV and 9 MeV, respectively, compared to homogenous water phantom.

The dose decreases of up to 21% (Figure 4b) were calculated behind the hip prosthesis for 18 MV due to high radiation absorption within the prosthesis and its shadowing effect. The shadowing effect causes the absorbed dose behind the prosthesis to fall down due to the dose absorption in the prosthesis [16]. This dose reduction behind the prosthesis should be considered when treatment planning to ensure the target tissue receives the prescribed dose. The increased dose in front of the prosthesis and the decreased dose behind the prosthesis's depth could result in the hot spot and cold spot region across the beamline, which is crucial to designing accurate dose planning. Placing high-density and atomic number prostheses in irradiated bone leads to soft tissue complications. Still, it can also potentially increase the risk of Osteoradionecrosis (ORN), often several years after initial radiation treatment [29].

According to a study by Toossi *et al.* (2013), the presence of CCM, stainless steel, Ti-alloy, and Ti prostheses caused an increase in electron contamination of 15 MV Siemens PRIMUS LINAC by factors of 1.18, 1.16, 1.16, and 1.14, respectively, as compared to when no prostheses were present [30]. From Table 2, our calculated EBF for 18 MV was a maximum of 1.34 for the Ti hip prosthesis and a minimum of 1.11 for the CCM hip prosthesis. No variation was reported in EBF with photon beam energy. For lower Z materials, EBF is constant up to 10 MV, then falls down. For higher Z materials, the EBF has a broad peak between 6 and 10 MV photon beams [1, 28]. By increasing electron beam energy, EBF was decreased [11, 31]. EBF is almost constant in a wide range of field sizes in photon beams [31], while for electron beams, it depends on field size [11]. From Table 3, for the 9 MeV beam, a dose perturbation of 40% was reported by Das *et al.* (2004) [32] for Ti is higher than the calculated value of 13.77% in our study. Our calculated dose perturbation for Ti, Ti-alloy, and SS prosthesis is more elevated than the reported data by Catli *et al.* (2013) [1]. The differences observed in the results of this study compared to other studies could be attributed to various factors, such as differences in experimental conditions and methods for measuring dose perturbation, including variations in the distance from the inhomogeneity interface, source-surface distance, field size, and the complexity of the geometry of the modeled inhomogeneity. The TPS could not accurately calculate the backscatter radiation resulting from metal prostheses. TPS underestimated the backscatter dose and overestimated the dose after the implants [1]. Our data confirm that it is essential to consider this dose perturbation due to the existence of the implant with a high atomic number and high density in the path of radiation to determine the dose distribution accurately.

5. Conclusion

The 2100 C/D Varian LINAC head for electron (9 MeV) and photon (18 MV) modes were modeled, and the dose distributions were successfully calculated with and without different hip prostheses. Our results show that the presence of hip prosthesis across the electron or photon beam line in radiotherapy perturbs the dose distribution from electron or photon beams. The EBFs depend on the density and atomic number of hip prosthesis and the type and energy of radiation. The increased dose in front of the prosthesis and the decreased dose behind the prosthesis's depth could result in the hot spot and cold spot region across the beam line, respectively; which is crucial to designing accurate dose planning. Considering this dose perturbation helps the planner adjust the radiotherapy treatment more precisely.

Acknowledgments

This study was supported financially by the Research Affairs of Ahvaz Jundishapur University of Medical Sciences, Ahvaz, Iran [Grant No. U-02169].

This article does not contain any studies with human or animal subjects performed by any of the authors.

The data that support the findings of this study are available upon reasonable request from the authors.

There is no use of animals or human subjects in this study.

This research received no specific grants from any funding agency in the public, commercial, or not-for-profit sectors.

References

1- Serap Çatli and Güneş Tanir, "Experimental and Monte Carlo evaluation of Eclipse treatment planning system for effects on dose distribution of the hip prostheses." *Medical Dosimetry,* Vol. 38 (No. 3), pp. 332-36, 2013/9// (2013).

2- Chester Reft *et al.*, "Dosimetric considerations for patients with HIP prostheses undergoing pelvic irradiation. Report of the AAPM Radiation Therapy Committee Task Group 63." *Medical Physics,* Vol. 30 (No. 6), pp. 1162-82, (2003).

3- George X. Ding and Christine W. Yu, "A study on beams passing through hip prosthesis for pelvic radiation treatment." *International Journal of Radiation Oncology Biology Physics,* Vol. 51 (No. 4), pp. 1167-75, (2001).

4- Edwige Buffard, Régine Gschwind, Libor Makovicka, and Céline David, "Monte Carlo calculations of the impact of a hip prosthesis on the dose distribution." *Nuclear Instruments and Methods in Physics Research, Section B: Beam Interactions with Materials and Atoms,* Vol. 251 (No. 1), pp. 9-18, (2006).

5- Kheirollah Mohammadi, Mohsen Hassani, Mahdi Ghorbani, Bagher Farhood, and Courtney Knaup, "Evaluation of the accuracy of various dose calculation algorithms of a commercial treatment planning system in the presence of hip prosthesis and comparison with Monte Carlo." *Journal of Cancer Research and Therapeutics,* (2017).

6- David W. H. Chin *et al.*, "Effect of dental restorations and prostheses on radiotherapy dose distribution: A monte carlo study." *Journal of Applied Clinical Medical Physics,* Vol. 10 (No. 1), pp. 80-89, (2009).

7- Paul J. Keall, Jeffrey V. Siebers, Robert Jeraj, and Radhe Mohan, "Radiotherapy dose calculations in the presence of hip prostheses." *Medical Dosimetry,* Vol. 28 (No. 2), pp. 107-12, (2003).

8- C. H. Sibata, H. C. Mota, P. D. Higgins, D. Gaisser, J. P. Saxton, and K. H. Shin, "Influence of hip prostheses on high energy photon dose distributions." *International Journal of Radiation Oncology, Biology, Physics,* Vol. 18 (No. 2), pp. 455-61, (1990).

9- M. Semlitsch and H. G. Willert, "Properties of implant alloys for artificial hip joints." *Medical & Biological Engineering & Computing,* Vol. 18 (No. 4), pp. 511-20, (1980).

10- M. Tatcher and S. Palti, "Evaluation of density correction algorithms for photon-beam dose calculations." *Radiology,* Vol. 141 (No. 1), pp. 201-05, (1981).

11- Nicholas Ade and F. C. P. du Plessis, "Measurement of the influence of titanium hip prosthesis on therapeutic electron beam dose distributions in a novel pelvic phantom." *Physica Medica,* Vol. 42pp. 99-107, 2017/10// (2017).

12- Sang Hoon Lee *et al.*, "Analysis of output factors with various detectors in small-field electron-beam radiotherapy." *Journal of the Korean Physical Society,* Vol. 60 (No. 5), pp. 875-80, (2012).

13- C. Glide-hurst, H. Zhong, M. Altman, D. Chen, and I. Chetty, "WE-C-BRB-01: Dosimetric Changes Realized from Extended Bit-Depth and Metal Artifact Reduction in CT." *Medical Physics,* Vol. 39 (No. 6), pp. 3943-43, (2012).

14- C. Coolens and P. J. Childs, "Calibration of CT hounsfield units for radiotherapy treatment planning of patients with metallic hip prostheses: The use of the extended CT-scale." *Physics in Medicine and Biology,* Vol. 48 (No. 11), pp. 1591-603, (2003).

15- Elinore Wieslander and Tommy Knöös, "Dose perturbation in the presence of metallic implants: Treatment planning system versus Monte Carlo simulations." *Physics in Medicine and Biology,* Vol. 48 (No. 20), pp. 3295-305, (2003).

16- Asghar Mesbahi and Farshad Seyed Nejad, "Dose attenuation effect of hip prostheses in a 9-MV photon beam: Commercial treatment planning system versus Monte Carlo calculations." *Radiation Medicine - Medical Imaging and Radiation Oncology,* Vol. 25 (No. 10), pp. 529-35, 2007/12// (2007).

17- Sung Yen Lin, Tieh Chi Chu, Jao Perng Lin, and Mu Tai Liu, "The effect of a metal hip prosthesis on the radiation dose in therapeutic photon beam irradiations." *Applied Radiation and Isotopes,* Vol. 57 (No. 1), pp. 17-23, (2002).

18- R. Roberts, "How accurate is a CT-based dose calculation on a pencil beam TPS for a patient with a metallic prosthesis?" *Physics in Medicine and Biology,* Vol. 46 (No. 9), pp. N227-N27, (2001).

19- Martin Erlanson, Lars Franzén, Roger Henriksson, Bo Littbrand, and Per olov Lofroth, "Planning of radiotherapy for patients with hip prosthesis." *International Journal of Radiation Oncology, Biology, Physics,* Vol. 20 (No. 5), pp. 1093-98, (1991).

20- P. J. Biggs and M. D. Russell, "Effect of a femoral head prosthesis on megavoltage beam radiotherapy." *International Journal of Radiation Oncology, Biology, Physics,* Vol. 14 (No. 3), pp. 581-86, (1988).

21- Brandon M. Barney, Ivy A. Petersen, Sean C. Dowdy, Jamie N. Bakkum-Gamez, Kristi A. Klein, and Michael G. Haddock, "Intraoperative Electron Beam Radiotherapy

(IOERT) in the management of locally advanced or recurrent cervical cancer." *Radiation Oncology*, Vol. 8 (No. 1), pp. 80-80, (2013).

22- Anuja Jhingran and Patricia J. Eifel, "Chapter 30 - The Endometrium." in *Radiation Oncology (Ninth Edition)*, James D. Cox and K. Kian Ang, Eds. Ninth Edit ed. Philadelphia: *Mosby*, (2010), pp. 774-97.

23- Daryoush Sheikh-Bagheri and D. W. O. Rogers, "Sensitivity of megavoltage photon beam Monte Carlo simulations to electron beam and other parameters." *medical physics*, Vol. 29 (No. 3), pp. 379-90, 2002/03/01 (2002).

24- Philip von Voigts-Rhetz, Damian Czarnecki, and Klemens Zink, "Effective point of measurement for parallel plate and cylindrical ion chambers in megavoltage electron beams." *Zeitschrift für Medizinische Physik*, Vol. 24 (No. 3), pp. 216-23, 2014/09/01/ (2014).

25- Jose Perez-Calatayud, Facundo Ballester, Miguel A. Serrano, José L. Lluch, Emilio Casal, and Vicente Carmona, "Dosimetric characteristics of backscattered electrons in lead." *Physics in Medicine & Biology*, Vol. 45 (No. 7), p. 1841, (2000).

26- Sanjay Sathiyan, M. Ravikumar, and Sanjay S. Supe, "Measurement of backscattered dose at metallic interfaces using high energy electron beams." *Reports of Practical Oncology and Radiotherapy*, Vol. 11 (No. 3), pp. 117-21, (2006).

27- D. Mihailescu and C. Borcia, "electron dose distributions in inhomogeneous phantoms: a Monte Carlo Study." *Rom. Rep. Phys*, Vol. 70pp. 603-03, (2018).

28- Indra J. Das and Faiz M. Kahn, "Backscatter Dose Perturbation at High Atomic Number Interfaces in Megavoltage Photon Beams." *Medical Physics*, Vol. 16 (No. 3), pp. 367-75, 1989/5// (1989).

29- Yang Li, Zhongsheng Zhou, Shenghao Xu, Jinlan Jiang, and Jianlin Xiao, "Review of the Pathogenesis, Diagnosis, and Management of Osteoradionecrosis of the Femoral Head." in Medical Science Monitor Vol. 29, ed, (2023).

30- Mohammad Taghi Bahreyni Toossi, Marziyeh Behmadi, Mahdi Ghorbani, and Hamid Gholamhosseinian, "A Monte Carlo study on electron and neutron contamination caused by the presence of hip prosthesis in photon mode of a 15 MV Siemens PRIMUS linac." *Journal of Applied Clinical Medical Physics*, Vol. 14 (No. 5), pp. 52-67, (2013).

31- Rowen J. de Vries and Steven Marsh, "Evaluation of backscatter dose from internal lead shielding in clinical electron beams using EGSnrc Monte Carlo simulations." *Journal of Applied Clinical Medical Physics*, Vol. 16 (No. 6), pp. 139-50, 2015/11// (2015).

32- Indra J. Das, Chee Wai Cheng, Raj K. Mitra, Alireza Kassaee, Zelig Tochner, and Lawrence J. Solin, "Transmission and dose perturbations with high-Z materials in clinical electron beams." *Medical Physics*, Vol. 31 (No. 12), pp. 3213-21, 2004/12// (2004).